

# Adaptive and Risk-Aware Target Tracking for Robot Teams with Heterogeneous Sensors

Siddharth Mayya<sup>1</sup>, Ragesh K. Ramachandran<sup>2</sup>, Lifeng Zhou<sup>1</sup>, Vinay Senthil<sup>1</sup>,  
Dinesh Thakur<sup>1</sup>, Gaurav S. Sukhatme<sup>2,3</sup>, Vijay Kumar<sup>1</sup>

**Abstract**—We consider a scenario where a team of robots with heterogeneous sensors must track a set of targets or hazards which may induce sensory failures on the robots. In particular, the likelihood of failures depends on the proximity between the targets and the robots. We propose a control framework that explicitly addresses the competing objectives of tracking quality maximization and sensor preservation (which impacts the future quality of the generated target estimates). Our framework consists of a risk-aware component—which accounts for the risk of suffering sensor failures, and an adaptive component—which balances the aforementioned competing objectives while accounting for failures that have already occurred. Based on a measure of the observability of the tracking process, our framework can generate aggressive as well as safer robot configurations to track the targets. Crucially, the heterogeneous sensing capabilities of the robots are explicitly considered at each step, allowing for a more expressive risk vs. tracking quality trade-off. Real robot experiments with induced sensor failures demonstrate the efficacy of the proposed approach.

## I. INTRODUCTION

Operating in disruptive environments is a fundamental requirement for achieving real-world autonomy in multi-robot systems. Consequently, a significant amount of research effort has been dedicated towards the design of multi-robot coordination algorithms which account for the presence of disturbances, e.g., [1], [2]. Broadly speaking, these approaches consist of two possible aspects: a *risk-aware* piece which generates solutions based on a model of the disturbance (typically interpreted as *robustness*) [3], or an *adaptive* piece which modifies the underlying control algorithm to continue task execution in spite of the disruptions affecting the system (a subset of such behaviors are referred to as *resilience*) [4]. The importance of both of these aspects depends on the mission objectives and can change during operations—while the latter prioritizes task performance, the former generates potentially conservative solutions to prevent future disruptions.

This research was sponsored by the Army Research Lab through ARL DCIST CRA W911NF-17-2-0181.

<sup>1</sup>S. Mayya, L. Zhou, V. Senthil, D. Thakur, and V. Kumar are with the GRASP Laboratory, University of Pennsylvania, Philadelphia, PA, USA {mayya, lfzhou, vinayksk, tdinesh, kumar}@seas.upenn.edu.

<sup>2</sup>R.K. Ramachandran and G.S. Sukhatme are with the Department of Computer Science, University of Southern California (USC), Los Angeles, CA, USA {rageshku, gaurav}@usc.edu.

<sup>3</sup>G.S. Sukhatme holds concurrent appointments as a Professor at USC and as an Amazon Scholar. This paper describes work performed at USC and is not associated with Amazon.

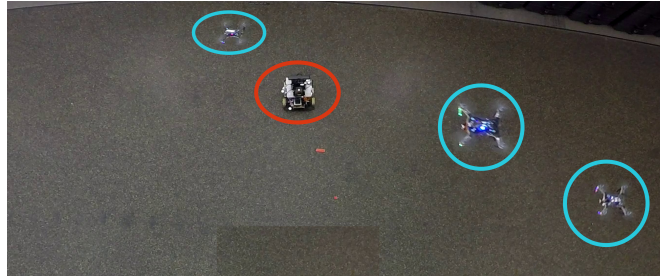


Fig. 1. A team of three aerial robots (marked by cyan ellipses) equipped with heterogeneous sensors tracks a ground robot target shown by the red ellipse (representing an adversary or an environmental hazard). The target is moving and can induce failures in the sensors of the robots based on the proximity between them. Therefore, the robots must position themselves close to the targets to generate accurate estimates, but must simultaneously account for the risk of failures.

These considerations are highly relevant in the context of heterogeneous multi-robot teams, where the different capabilities of the robots can be leveraged to magnify the efficacy of the robot team [5]. For example, if only a single robot in the multi-robot team carries an essential sensor required for the success of the task, this robot should take less risky actions compared to other robots which carry non-essential sensors. The central question then is: *How should one systematically balance the objectives of risk-awareness and performance-maximization in heterogeneous multi-robot teams?*

In the context of a target tracking application, this paper presents a framework which synthesizes adaptive and risk-aware poses for a team of robots equipped with heterogeneous sensing capabilities. We consider a team of robots tracking mobile adversarial targets in a failure-prone and harsh environment. Here “target” can refer to an adversarial agent [6] or hazardous environmental elements such as fires or nuclear hazards [7]. The robots are equipped with different types of sensors and are tasked with estimating the states of the targets. Each type of sensor measures different projections of the target states e.g., [8]. In addition to the sensors being noisy, the targets are moving and can induce failures in the sensors of the robots based on the proximity between them. In such a scenario, the robots must not only position themselves in order to achieve a trade-off between risk and tracking quality, they must also suitably adapt to failures that have rendered certain sensors dysfunctional.

Towards this end, we formulate an optimization problem

whose solutions drive the team of robots to track the targets in a risk-aware manner. We present a novel mechanism to encode risk-awareness in a multi-robot system equipped with heterogeneous sensors. This involves composing a safety-aware observability Gramian (SOG) matrix, which weighs the quality of future observations made by the multi-robot team with the risk of failures associated with making those observations. By encoding the robots' heterogeneous sensors within the SOG, our framework positions robots based on the risk-weighted contribution of their sensors to the overall tracking performance. Illustrative examples as well as real robot experiments demonstrate the salient features of this framework.

Leveraging concepts from structural and dynamic observability theory [9], our framework automatically trades between the objectives of risk-awareness and tracking performance maximization by considering the *sensing margin*—defined as the relative observability of the target tracking system when compared to a failure-free scenario. As illustrated in Fig. 2, this enables our algorithm to prioritize tracking quality when the sensing margin is large and switch to non-risky behaviors as the sensing margin of the team decreases.

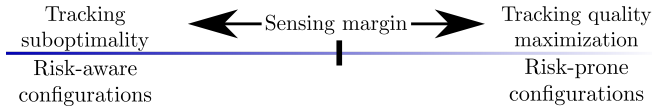


Fig. 2. The framework proposed in this paper enables a systematic trade-off between tracking quality and the overall risk (of sensing failures) taken by the target tracking robots.

It should be noted at this point that the developed framework is centralized and does not computationally scale particularly well for large teams of robots. However, these limitations should be understood in light of the ultimate ambition of this paper, which is to illustrate how heterogeneity in the robot team can be explicitly leveraged to enhance risk-aware and adaptive behaviors in multi-robot teams. Furthermore, the developed framework can be utilized in the pre-mission planning stage to evaluate the efficacy of various sensor configurations towards accomplishing the mission objectives.

## II. LITERATURE REVIEW

Safety-aware target tracking typically requires modeling the uncertain target dynamics, designing an uncertainty-regulating control algorithm, and fusing it with a risk-aware control piece, e.g., [10], [11]. For instance, [12], [13] develop wildfire tracking algorithms for multi-robot teams, which leverage specialized estimation algorithms to model the state of fires and firefighters. In these works, artificial potential fields are leveraged as the primary safety-aware control piece, applying a force on the robots if they get too close to danger. Safety barrier certificates provide another mechanism to achieve similar safety behaviors [14]. [7] considers a multi-robot mapping scenario in the presence of hazards, and uses a mutual information approach to

achieve a trade-off between sensor preservation and taking quality measurements. In this paper, we assume that the risk-fields associated with the target tracking process are known. Our main focus is exploiting heterogeneity in the available sensors to actively trade off potential risk with tracking performance, as summarized in Fig. 2.

Given the complexity of balancing performance and safety objectives especially in complex environments, data-driven approaches to coverage and tracking have been designed, e.g., [15], [16]. In particular, [17] designs a reinforcement learning algorithm for tracking an evolving wildfire using a team of robots. Here, the robots are tasked with strategically applying fire retardant in order to contain the fire. Typical concerns with such approaches revolve around generalizability to new scenarios and the difficulties in reward shaping, as well as generating tuned and interpretable results.

As disruptions are inevitable during the long duration operations of robot teams, mechanisms to maintain performance despite failures have been developed e.g., [18], [19], [20]. In the context of target tracking, [19] develops a mechanism to reconfigure the communication network of the robot team in order to compensate for resource failures.

## III. PROBLEM SETUP

This section formally introduces the heterogeneous sensing model of the multi-robot team and sets up the risk-aware target tracking problem. We also introduce the target-induced sensor failure models, which will be used in Section IV to imbue risk-awareness into the proposed controller.

### A. Notation

In this paper capital letters are used to represent matrices and small letters indicate either scalars or vectors. Additionally, bold letters are used to represent vectors or matrices. For any positive integer  $z \in \mathbb{Z}^+$ ,  $[z]$  denotes the set  $\{1, 2, \dots, z\}$ .  $\|\cdot\|_p$  denotes the  $p$ -norm and the induced  $p$ -norm for vectors and matrices, respectively (subscripts are dropped for the 2-norm).  $\mathbf{1}^{m_1}$  and  $\mathbf{1}^{m_1 \times m_2}$  denote a vector and matrix of ones, respectively.  $\mathbf{I}_m$  denotes the identity matrix of size  $m \times m$ . The operator  $|\cdot|$  denotes either the length of a vector or the cardinality of a set. Given a vector  $\mathbf{v}$ ,  $\text{Diag}(\mathbf{v})$  represents a diagonal matrix with elements of  $\mathbf{v}$  along its diagonal. Also,  $\text{Tr}(\mathbf{M})$  results in the trace of  $\mathbf{M}$ . Given a set of matrices  $\{\mathbf{M}_1, \mathbf{M}_2, \dots, \mathbf{M}_n\}$ ,  $[\mathbf{M}_1, \mathbf{M}_2, \dots, \mathbf{M}_n]$  and  $[\mathbf{M}_1; \mathbf{M}_2; \dots, \mathbf{M}_n]$  represent the matrices obtained through horizontal and vertical concatenation of the given matrices, respectively. Furthermore,  $\mathbf{M}_1 \oplus \mathbf{M}_2 \oplus \dots \oplus \mathbf{M}_n$  yields a block diagonal matrix of constituent matrices and  $\mathbf{M}_1 \otimes \mathbf{M}_2$  denotes the Kronecker product.

### B. Problem Formulation

Consider  $N$  robots equipped with a set of heterogeneous sensors, whose configurations and noise models are described in Section III-C and III-D. Additionally, consider  $M$  targets whose dynamics are described in Section III-D and which induce sensing failures on the robots according to the risk fields specified in Section III-E.

At each point in time  $t = 1, 2, \dots, T$ , we are interested in computing desired goal states for the robots which meet the following objectives:

- 1) the robots generate estimates of the targets' positions with a *tracking error* lower than a given threshold;
- 2) the *risk* of taking these measurements is upper bounded by a given threshold;
- 3) the first two objectives are achieved while accounting for the heterogeneity in the sensing capabilities of the robots as well as sensing failures which have already occurred.

### C. Robot Team Model

Consider a team of  $N$  robots engaged in the target tracking task, indexed by the set  $\mathcal{R} := [N]$ . Let  $\mathbf{x}_{i,t} \in \mathcal{X} \subseteq \mathbb{R}^p$  denote the state of robot  $i$  at discrete time  $t$ , and  $\mathbf{u}_{i,t} \in \mathcal{U} \subseteq \mathbb{R}^q$  denote its control input, which steers the state according to the following control-affine dynamics:

$$\mathbf{x}_{i,t} = f(\mathbf{x}_{i,t-1}) + g(\mathbf{x}_{i,t-1})\mathbf{u}_{i,t-1}, \quad t = 1, 2, \dots \quad (1)$$

where  $f : \mathbb{R}^p \rightarrow \mathbb{R}^p$  and  $g : \mathbb{R}^p \rightarrow \mathbb{R}^{p \times q}$  are continuously differentiable vector fields. For simplicity of analysis, we assume that the robots are perfectly localized and we do not explicitly model any process noise in the dynamics of the robots. However, the developed framework can be extended to account for such a scenario.

The robots are equipped with a set of heterogeneous sensors for tracking targets in the environment. Let  $U$  denote the number of distinct types of sensors available within the team. Let  $\mathbf{\Gamma}_t \in \{0, 1\}^{U \times N}$  denote the *sensor matrix* which describes the distribution of sensors over the robot team at time  $t$ :

$$\mathbf{\Gamma}_{si,t} = \begin{cases} 1, & \text{if robot } i \text{ has sensor } s \text{ at time } t, \\ 0, & \text{otherwise.} \end{cases} \quad (2)$$

Note that target-induced sensor failures might modify the sensor matrix, hence it's explicit time dependence.

### D. Target Tracking

The robots are tasked with tracking a set of  $M$  targets in the environment, which are indexed by the set  $\mathcal{T} := [M]$ . Let  $\mathbf{z}_{j,t} \in \mathcal{X} \subseteq \mathbb{R}^p$  denote the state of target  $j \in \mathcal{T}$  at time  $t$ , whose motion in the environment is described by the linear dynamics:  $\mathbf{z}_{j,t} = \mathbf{A}_j \mathbf{z}_{j,t-1} + \mathbf{B}_j \mathbf{u}_{j,t-1}^z + \mathbf{w}_{j,t-1}^z$ , where  $\mathbf{A}_j \in \mathbb{R}^{p \times p}$  and  $\mathbf{B}_j \in \mathbb{R}^{p \times q}$  are the process and control matrices,  $\mathbf{w}_{j,t}^z \in \mathbb{R}^p$  is the zero-mean independent Gaussian noise with a covariance matrix  $\mathbf{Q}_j \in \mathbb{R}^{p \times p}$ , and  $\mathbf{u}_{j,t}^z \in \mathcal{U} \subseteq \mathbb{R}^q$  is the control input of target  $j \in \mathcal{T}$  at time  $t$ . Stacking the target states and target control inputs into the vectors  $\mathbf{z}_t$  and  $\mathbf{u}_t^z$ , respectively, we get:

$$\mathbf{z}_t = \mathbf{A} \mathbf{z}_{t-1} + \mathbf{B} \mathbf{u}_{t-1}^z + \mathbf{w}_{t-1}^z, \quad (3)$$

where  $\mathbf{A} \triangleq \mathbf{A}_1 \oplus \dots \oplus \mathbf{A}_M$ ,  $\mathbf{B} \triangleq \mathbf{B}_1 \oplus \dots \oplus \mathbf{B}_M$ , and  $\mathbf{w}_t^z \triangleq [\mathbf{w}_{1,t}^z; \dots; \mathbf{w}_{M,t}^z]$ . As described before, we let  $\mathbf{w}_t^z \sim \mathcal{N}(0, \mathbf{Q})$ ,  $\mathbf{Q} \triangleq \mathbf{Q}_1 \oplus \mathbf{Q}_2 \oplus \dots \oplus \mathbf{Q}_M$ .

Within our framework, every robot  $i$  makes an observation of every target  $j$  according to the following linear observation model:

$$\mathbf{y}_{ij,t} = \mathbf{H}_{ij,t} \mathbf{z}_{j,t} + \boldsymbol{\nu}_{ij,t}, \quad i \in \mathcal{R}, \quad j \in \mathcal{T}, \quad (4)$$

where  $\mathbf{y}_{ij,t}$  is the measurement,  $\boldsymbol{\nu}_{ij,t}$  is the measurement noise, and  $\mathbf{H}_{ij,t}$  is the measurement matrix corresponding to robot  $i$ 's measurements of target  $j$  and will depend on the sensor suite available to robot  $i$  at time  $t$ .

Let  $\gamma_{i,t} = [s \in [U] \mid \mathbf{\Gamma}_{si,t} = 1]$  denote the vector containing the ordered row indices of the sensor matrix (2) corresponding to robot  $i$ . In this paper, we associate a one-dimensional output matrix corresponding to each sensor available in the team, denoted by the set  $\mathcal{S} := \{\mathbf{h}_1, \dots, \mathbf{h}_U\}$ . Consequently, the measurement matrix for robot  $i$  associated with the process of taking measurements about the state of target  $j$  at time  $t$  can be constructed simply using the set  $\mathcal{S}$  and  $\gamma_{i,t}$ ,

$$\mathbf{H}_{ij,t} = [\mathbf{h}_{\gamma_{i,t}(1)}; \dots; \mathbf{h}_{\gamma_{i,t}(|\gamma_{i,t}|)}]. \quad (5)$$

We model the measurement noise  $\boldsymbol{\nu}_{ij,t} \sim \mathcal{N}(0, \mathbf{R}_{ij,t})$  to be zero-mean, independent, and Gaussian whose covariance  $\mathbf{R}_{ij,t}$  is distance dependent, and exponentially increases with the distance between the robots and the targets,

$$\mathbf{R}_{ij,t}^{-1} = \text{Diag}([R_{ij1,t}^{-1}, R_{ij2,t}^{-1}, \dots, R_{ij|\gamma_{i,t}|,t}^{-1}]) \quad (6)$$

with

$$\mathbf{R}_{ijs,t}^{-1} = w_s \exp(-\lambda_s \|\mathbf{x}_{i,t} - \mathbf{z}_{j,t}\|), \quad \forall s \in [|\gamma_{i,t}|], \quad (7)$$

where  $\lambda_s$  and  $w_s$  determine the noise characteristics of each sensor  $s$  in the sensor suite of robot  $i$ . While this paper chooses an exponential decay model to capture the sensor performance characteristics, any other continuously differentiable degradation function can be utilized instead.

In ensemble form, the measurements of all the targets by robot  $i$  can be written as  $\mathbf{y}_{i,t} = \mathbf{H}_{i,t} \mathbf{z}_t + \boldsymbol{\nu}_{i,t}$ ,  $\forall i \in \mathcal{R}$ , where  $\mathbf{H}_{i,t} = \mathbf{I}_M \otimes \mathbf{H}_{ij,t}$ , and  $\boldsymbol{\nu}_{i,t} = [\boldsymbol{\nu}_{i1,t}; \dots; \boldsymbol{\nu}_{iM,t}]$ . Here  $\mathbf{I}_M$  denotes the identity matrix of size  $M$ . The measurement equation for the team can be written as:

$$\mathbf{y}_t = \mathbf{H}_t \mathbf{z}_t + \boldsymbol{\nu}_t, \quad (8)$$

where  $\mathbf{y}_t = [\mathbf{y}_{1,t}; \mathbf{y}_{2,t}; \dots; \mathbf{y}_{N,t}]$ ,  $\mathbf{H}_t = [\mathbf{H}_{1,t}; \mathbf{H}_{2,t}; \dots; \mathbf{H}_{N,t}]$  and  $\boldsymbol{\nu}_t = [\boldsymbol{\nu}_{1,t}; \boldsymbol{\nu}_{2,t}; \dots; \boldsymbol{\nu}_{N,t}]$ . The team-wise measurement noise can be written as  $\boldsymbol{\nu}_t \sim \mathcal{N}(0, \mathbf{R}_t)$  where  $\mathbf{R}_t = \mathbf{R}_{11,t} \oplus \mathbf{R}_{12,t} \oplus \dots \oplus \mathbf{R}_{NM,t}$ . Thus, given a sensor matrix  $\mathbf{\Gamma}_t$  and the available sensor bank  $\mathcal{S}$ , one can construct the corresponding robot output matrix and hence the team output matrix. The following example illustrates a potential configuration of sensors on robots using the above defined terminology.

*Example 1:* Consider two robots  $r_1$  and  $r_2$  equipped with three types of sensors (denoted  $s_1, s_2, s_3$ ) whose sensor configuration matrix as well as linear measurement matrices

are given by:

$$\mathbf{h}_1 = [1 \ 0], \mathbf{h}_2 = [0 \ 1], \mathbf{h}_3 = [1 \ 1], \quad (9)$$

$$\mathbf{\Gamma}^\top = \begin{matrix} & s_1 & s_2 & s_3 \\ \begin{matrix} r_1 \\ r_2 \end{matrix} & \begin{pmatrix} 1 & 0 & 0 \\ 1 & 1 & 1 \end{pmatrix} \end{matrix}. \quad (10)$$

As seen, sensors  $s_1$  and  $s_2$  measure the x- and y- coordinates of the targets, respectively, and sensor  $s_3$  returns a linear combination of both values.

#### E. Target-induced Risk Model

As discussed in the introduction, each target can induce failures within the robot team. Let  $\phi_j : \mathcal{X} \rightarrow [0, 1]$  represent the *target risk field* which models the probability of a robot experiencing a sensing failure caused by target  $j \in \mathcal{T}$ . In particular,  $\phi_j(\mathbf{x}_{i,t})$  represents this failure probability for robot  $i$  with state  $\mathbf{x}_{i,t}$ . In addition, we define the *safety field*  $\pi_j : \mathcal{X} \rightarrow \mathbb{R}^+$  associated with  $\phi_j(\mathbf{x}_{i,t})$  as

$$\pi_j(\mathbf{x}_{i,t}) = -\log(\phi_j(\mathbf{x}_{i,t})). \quad (11)$$

Note that,  $\pi_j$  increases with a decrease in  $\phi_j$ . Thus, the safety field  $\pi_j$  encodes the safety of a robot in the vicinity of target  $j$ . Intuitively, it quantifies the ability of robot  $i$  to survive failure from target  $j$  while residing at  $\mathbf{x}_{i,t}$ . Depending on the context, we refer to this model as either the risk model or the safety model. Furthermore, we assume that the functional form of the target risk fields are known to the robot team (see Section V for particular choices of these functions), and that robots can detect the health of their own sensors [21].

### IV. ADAPTIVE AND RISK-AWARE TARGET TRACKING

Given the measurements of the targets as well as the risk model, this section first mathematically describes the technique used to generate estimates of the target locations. Subsequently, we introduce the *safety-aware observability Gramian* (SOG) to explicitly weigh the information provided by measurements against the risk incurred while taking them. We then formulate the optimization program for generating the desired positions of the robots.

#### A. Generating Target Estimates

To address the target tracking problem, we employ a Kalman filter to generate a sequence of optimal estimates (at each time  $t$ ) of the states of all targets  $\hat{\mathbf{z}}_t$  along with the covariance matrix  $\mathbf{P}_t$ , which signifies the confidence in the generated estimate. Typically, the Kalman filter operations consist of prediction and update steps. In the prediction step, we have,

$$\hat{\mathbf{z}}_{t,-} = \mathbf{A}\hat{\mathbf{z}}_{t-1}, \quad \mathbf{P}_{t,-} = \mathbf{A}\mathbf{P}_{t-1}\mathbf{A}^\top + \mathbf{Q}, \quad (12)$$

where  $\hat{\mathbf{z}}_{t,-}$  and  $\mathbf{P}_{t,-}$  are (a priori) estimated states of all the targets and the corresponding (a priori) covariance matrix at the next step, respectively;  $\hat{\mathbf{z}}_{t-1}$  and  $\mathbf{P}_{t-1}$  are the estimated states of the targets and the team-wise covariance matrix at the previous time step, respectively; and  $\mathbf{Q}$  is the process noise covariance, defined after (3). Once the robots'

measurements  $\mathbf{y}_t$  (defined in (8)) are available, we have the Kalman filter update step as,

$$\hat{\mathbf{z}}_t = \hat{\mathbf{z}}_{t,-} + \mathbf{K}_t \tilde{\mathbf{y}}_t, \quad \mathbf{P}_t = (\mathbf{I} - \mathbf{K}_t \mathbf{H}_t) \mathbf{P}_{t,-}, \quad (13)$$

where  $\hat{\mathbf{z}}_t$  and  $\mathbf{P}_t$  are the (a posteriori) estimated states of the targets and the (a posteriori) team-wise covariance matrix at the next step;  $\tilde{\mathbf{y}}_t := \mathbf{y}_t - \mathbf{H}_t \hat{\mathbf{z}}_{t,-}$  is measurement pre-fit residual;  $\mathbf{K}_t := \mathbf{P}_{t,-} \mathbf{H}_t^\top (\mathbf{H}_t \mathbf{P}_{t,-} \mathbf{H}_t^\top + \mathbf{R}_t)^{-1}$  is the Kalman gain with  $\mathbf{R}_t$  denoting the measurement noise covariance matrix, as described in (8). Notably, the team-wise (a posteriori) covariance matrix  $\mathbf{P}_t$  can be expressed as  $\mathbf{P}_t = \mathbf{P}_{1,t} \oplus \mathbf{P}_{2,t} \oplus \dots \oplus \mathbf{P}_{M,t}$  with  $\mathbf{P}_{j,t}$  denoting the (a posteriori) covariance matrix corresponding to all robots' joint estimate of target  $j \in \mathcal{T}$  at time  $t$ .

#### B. Imparting Risk-aware Behaviors

The trade-off between risk and measurement quality is made non-trivial by the fact that sensors from different agents might be required to ensure that the target system is observable, and thus, certain robots might be more “valuable” to the team than others. This notion is formally described by the *observability Gramian* [22], which, for the multi-robot team tracking the targets (at time  $t$ ) is defined as:  $\mathbf{O}_t \triangleq \sum_{k=0}^{T_o-1} (\mathbf{A}^\top)^k \mathbf{H}_t^\top \mathbf{H}_t (\mathbf{A})^k$ , where  $T_o \geq 0$  is a suitably chosen time horizon. In this computation, we make the simplifying assumption that the sensor matrix  $\mathbf{H}_t$  remains constant over the time horizon  $T_o$ . As will be demonstrated in Section IV-D, this assumption allows the robots to effectively track the targets while also accounting for sensor failures as they happen.

The positive definiteness of  $\mathbf{O}_t$  is a necessary and sufficient condition for the observability of a deterministic linear system [22], which guarantees that the initial state of the system can be reconstructed from subsequent measurements and knowledge of the control inputs of the observed system. In particular, it should be noted that *a measure of the observability Gramian (such as the trace) can serve as a proxy for the ease of estimating the states of the observed system from future measurements* e.g., [9], [23].

In our scenario, proximity between the robots and the targets will prove detrimental to the ability of the robots to sense the targets in the future, due to the increasing risk of target-induced sensor failures. To encode this objective, our paper introduces a novel weighted observability Gramian, expressed as:

$$\mathbf{O}_{\Pi,t} \triangleq \sum_{k=0}^{T_o-1} (\mathbf{A}^\top)^k \mathbf{H}_t^\top \mathbf{\Pi}_t \mathbf{H}_t (\mathbf{A})^k, \quad (14)$$

where  $\mathbf{\Pi}_t$  is a positive definite matrix quantifying the *inverse* of the risk (of sensor failures) corresponding to the different robots. As the risk model described in Section III-E is purely dependent on the states of the targets and the robots, we can define  $\mathbf{\Pi}_t$  as,

$$\mathbf{\Pi}_t = \oplus_{i=1}^N \left( \bigoplus_{j=1}^M \mathbf{I}_{|\gamma_{i,t}|} \otimes \pi_j(\mathbf{x}_{i,t}) \right) \quad (15)$$



where  $\pi_j(\mathbf{x}_{i,t})$  is the safety field with respect to robot  $i$  and target  $j$ , as defined in (11), and the operators  $\oplus$  and  $\otimes$  are defined in Section III-A. Note that, the block diagonal matrices  $\mathbf{I}_{|\gamma_{i,t}|} \otimes \pi_j(\mathbf{x}_{i,t})$  which compose the matrix  $\mathbf{\Pi}_t$  represent the inverse risk associated with the proximity between target  $j$  and robot  $i$ . In other words, *larger the diagonal entries of  $\mathbf{O}_{\mathbf{\Pi},t}$ , larger is the ability of the robot team to obtain the targets' state measurements while surviving sensor failures*. Thus, we refer to the matrix  $\mathbf{O}_{\mathbf{\Pi},t}$ —composed by modifying the observability Gramian  $\mathbf{O}_t$ —as the safety-aware observability Gramian (SOG) matrix. The following example illustrates the ability of the SOG to quantify risk in this setting.

*Example 2:* Consider two robots  $r_1$  and  $r_2$  equipped with the sensor configuration defined in Example 1. As seen, robot  $r_2$  is equipped with more sensors than robot  $r_1$ , and ensures that the overall tracking system is observable (which requires obtaining both the x- and y- coordinates of the target). The target risk field is chosen as a Gaussian function centered on the target (we omit the details for brevity). With the target placed at  $[2; 2]$ , we consider two different configurations of the robots relative to the target and evaluate the trace of the inverse SOG matrix for these two scenarios: Case 1:  $\mathbf{x}_1 = [1; 1]$ ,  $\mathbf{x}_2 = [0; 0]$ , Case 2:  $\mathbf{x}_1 = [0; 0]$ ,  $\mathbf{x}_2 = [1; 1]$ . As expected,  $\text{Tr}(\mathbf{O}_{\mathbf{\Pi},t}^{-1})$  was greater in case 2 (0.40) than in case 1 (0.37). This is primarily because case 2 presents a “riskier” configuration where the robot contributing more towards the tracking performance (robot 2) is placed closer to the target, thus effectively reducing the future tracking quality of the system. This demonstrates the ability of the SOG matrix to quantify the risk-weighted tracking quality of the heterogeneous sensor system.

In the optimization problem described in Section IV, we bound the trace of  $\mathbf{O}_{\mathbf{\Pi},t}^{-1}$  from above to bound the failure risk of the robot team.

### C. Sensing Margin

We explicitly trade-off between tracking quality maximization and risk-awareness based on a quantification of the abundance and diversity of sensors available in the team. Consider the linear system defined by the dynamics in (3) and sensing model in (8). From linear system theory [22], we know that the pair  $(\mathbf{A}, \mathbf{H}_t)$  is observable if and only if  $\mathcal{O} = [\mathbf{H}_t; \mathbf{H}_t\mathbf{A}; \mathbf{H}_t\mathbf{A}^2; \dots; \mathbf{H}_t\mathbf{A}^{\varphi-1}]$  has rank  $\varphi$ , where  $\varphi = Mp$ . Furthermore, the eigenvalues of the matrix  $\mathcal{O}^\top \mathcal{O}$  also provide information regarding how close the system is to becoming unobservable, which enables system designers to compare candidate observable systems [23]. Inspired by the conditioning numbers introduced in [9], we define the *sensor margin*  $\eta_t$  at time  $t$  as the maximum eigenvalue of  $\mathcal{O}^\top \mathcal{O}$  if the overall system is observable:

$$\eta_t = \begin{cases} \lambda_{\max}(\mathcal{O}^\top \mathcal{O}), & \text{if } \lambda_{\min}(\mathcal{O}^\top \mathcal{O}) \neq 0, \\ 0, & \text{otherwise.} \end{cases} \quad (16)$$

As discussed above, larger the maximum eigenvalue of  $\mathcal{O}^\top \mathcal{O}$ , the farther the system is from being unobservable owing to both the *diversity* and *abundance* of available

sensors. This definition of the sensor margin  $\eta_t$  will be leveraged in the optimization program defined in the next section.

### D. Optimization Problem

We propose solving the following optimization program to obtain the states of the robots for target tracking. As seen from (17a), the primary objective of the optimization problem is to minimize slack variables  $\delta_1$  and  $\delta_2$  which represent the suboptimality in the tracking performance as well as the risk mitigation, respectively. As we explain in the following, this ensures that the dual intent of tracking performance maximization and sensor preservation are satisfied. Note that, for clarity of notation, the subscript for time dependence has been omitted for this subsection.

### Adaptive and Risk-Aware Target Tracking (17)

$$\underset{\mathbf{x}, \delta_1, \delta_2}{\text{minimize}} \quad q_1 \eta \|\delta_1\|_1 + q_2 \frac{1}{1 + \eta} \delta_2^2, \quad (17a)$$

$$\text{s.t.} \quad \|\mathbf{x}_i - \bar{\mathbf{x}}_i\| \leq d_m, \quad \forall i \in \mathcal{R}, \quad (17b)$$

$$\|\mathbf{x}_i - \mathbf{x}_j\| \geq d_n, \quad \forall i \neq j, \quad \forall i, j \in \mathcal{R}, \quad (17c)$$

$$\text{Tr}(\mathbf{P}_j) \leq \rho_{1,j} + \delta_{1,j}, \quad \delta_{1,j} \geq 0, \quad j \in \mathcal{T}, \quad (17d)$$

$$\text{Tr}(\mathbf{O}_{\mathbf{\Pi}}^{-1}) \leq \rho_2 + \delta_2, \quad \delta_2 \geq 0, \quad (17e)$$

where  $\bar{\mathbf{x}}_i$  is robot  $i$ 's state at the current time step  $t$ ,  $\mathbf{x} := [\mathbf{x}_1^\top; \mathbf{x}_2^\top; \dots; \mathbf{x}_N^\top]$  is the optimization variable representing the ensemble state of all robots at the next time step  $t+1$ ,  $d_m$  is the maximum distance each robot  $i$  can move between two consecutive time steps, and  $d_n$  is the minimum inter-robot distance for safety. Furthermore,  $\rho_1 = [\rho_{1,1}; \rho_{1,2}; \dots; \rho_{1,M}]$  and  $\rho_2$  denote the user-defined upper bounds on the tracking error (encoded by  $\mathbf{P}$ ) and team-level risk (encoded by  $\mathbf{O}_{\mathbf{\Pi}}^{-1}$ ), respectively (see problem description in Section III-B).

The pertinent aspects of the above described formulation are encoded in constraints (17d) and (17e) as well as the objective (17a). Equation 17d nominally aims to bound the trace of the posterior covariance matrix  $\mathbf{P}_j$  (13) for each target  $j$  by a constant  $\rho_{1,j}$ . However, sensor failures might imply that meeting this performance criteria is not longer possible. To this end, the slack variable  $\delta_1 := [\delta_{1,1}; \delta_{1,2}; \dots; \delta_{1,M}]$  imparts a “*bend but not break*” behavior to the framework ensuring that it adapts to the current operating conditions. Similarly, the risk of sensor failures is captured by the inverse SOG  $\mathbf{O}_{\mathbf{\Pi}}^{-1}$  and it is upper bounded by the sum of  $\rho_2$  and the slack variable  $\delta_2$ , denoting adjustments to the prescribed safety margins (17e).

We now describe the intuition behind the minimized expression in (17a). Generally speaking, with fewer heterogeneous sensors (i.e., a lower  $\eta$ ), the robot team should lower its expectations on the tracking performance by choosing a larger  $\|\delta_1\|_1$  (in (17d)) and prioritize safety by choosing a smaller  $\delta_2$  (in (17e)). Conversely, with more heterogeneous sensors, the robots should aim to achieve a higher tracking quality by choosing a smaller  $\|\delta_1\|_1$  and can be more risk-seeking by choosing a larger  $\delta_2$ . The cost function (17a) reflects this relationship by penalizing the slack terms based

on the sensing margin  $\eta$  (along with scaling factors  $q_1$  and  $q_2$ ). This allows the framework to adaptively prioritize risk-awareness and performance maximization based on the sensing margin  $\eta$ .

Equation 17b limits the distance that each robot can travel between two consecutive steps. Equation 17c guarantees that the generated solutions maintain a minimum safety distance between the robots. It should be noted that  $\mathbf{P}$  is computed directly using the update equation (13) and  $\mathbf{O}_\Pi$  is computed using the estimated state of the targets  $\hat{\mathbf{z}}$  computed in (14). It should be noted that, the complete failure of a robot in the team can be modeled by solving the same optimization problem but with a different set of parameters (number of robots, sensor configuration, etc).

### E. Computational Aspects

The optimization problem (17) can be solved at each time  $t \in \mathbb{N}$  based on the updated estimates of the target states. Algorithm 1 illustrates the operations of the target tracking framework. Step 3 uses the Kalman filter to generate estimates of the target positions. Using this estimate, Step 4 generates new positions for the robots according to the tradeoffs between tracking performance maximization and risk-awareness. In Section V, we use a simple proportional-integral controller to drive the robots towards these desired positions. Following this, the robots evaluate which of their sensors have failed due to proximity with the targets, and update the sensing margin in Step 7. In particular, we solve the non-linear non-convex optimization problem given in (17) using SNOPT [24] via pydrake [25]. This entails a trade-off between solve time and the resulting sub-optimality of the generated solutions. We warm-start the solver with the solution from the previous iteration in order to improve the quality of generated solutions as well as reduce solve time.

---

#### Algorithm 1 Adaptive and Risk-Aware Target Tracking

---

Target and Team Specs:  $N, M, \phi_j, w_l, \lambda_l, \Gamma_0, \mathbf{H}_0$   
Parameters:  $\rho_1, \rho_2, q_1, q_2, d_m, d_n$

- 1: Initialize:  $t = 0$
- 2: **while** true **do**
- 3:   Update target position estimate  $\hat{\mathbf{z}}_t$   $\triangleright$  (13)
- 4:   Execute the adaptive risk-aware controller  $\triangleright$  (17)
- 5:   Drive the robots towards the desired configuration
- 6:   Compile sensor failures and update  $\Gamma_t$
- 7:   Update sensing margin  $\eta_t$   $\triangleright$  (16)
- 8:    $t = t + 1$
- 9: **end while**

---

## V. EXPERIMENTAL EVALUATION

In this section, we present a series of real as well as simulated experiments which demonstrate the ability of the proposed framework to track multiple targets in an adaptive and risk-aware manner. The target risk field  $\phi_j$  corresponding to the target  $j \in \mathcal{T}$  is modeled to increase with proximity (e.g., to model failure risk from fires, nuclear hazards, etc)

and is described by a Gaussian function centered around the target,

$$\phi_j(\mathbf{x}) = \frac{c_j}{2\pi|\Sigma_j|} \exp\left(-\frac{1}{2}(\mathbf{x} - \mathbf{z}_j)^\top \Sigma_j(\mathbf{x} - \mathbf{z}_j)\right), \quad (18)$$

where  $c_j$  determines the peak value of the field for target  $j$ , and  $\Sigma_j$  determines the variance.

We consider three Dragonfly 230 quadrotors [26] equipped with three different types of sensors, whose reduced measurement matrices are given by (9). The quadrotors use on-board visual-inertial odometry to localize themselves and communicate their positions to the central computer. In this experiment, the central computer synthesizes noisy measurements of the targets as well as simulates the sensor failures based on the distance between the target (a Scarab ground robot [27]) and the quadrotors. The waypoints generated by solving the optimization program (computed in a 2D plane with a fixed elevation) are transmitted from the central computer to the quadrotors via ROS.

The sensor matrix of the robots at deployment time is specified as  $\Gamma_0 = \mathbf{1}^{3 \times 3}$ . The target risk field parameters are chosen as  $c_1 = 0.4$  and  $\Sigma_1 = \text{Diag}([2.0, 2.0])$ . Sensor failures on the robots are simulated by flipping a biased coin proportional to the magnitude of the target risk field at the robot's location. While the true state of the target  $\mathbf{z}_t$  is used to simulate the failures, the robots compute  $\mathbf{O}_\Pi$  using the estimated state of the targets  $\hat{\mathbf{z}}_t$  as they do not have access to the true target states.

The sensor parameters are chosen as  $w_s = 1.80, \lambda_s = 0.1, \forall s \in \{1, 2, 3\}$ , and the target dynamics are set to  $\mathbf{A}_1 = \text{Diag}([1, 1]), \mathbf{B}_1 = \text{Diag}([1, 1])$ . Unknown target dynamics can also be identified using measurements via online system identification techniques [28]. For the parameters ( $d_m = 20.0, d_n = 0.9, \rho_1 = [0.001, 0.001], \rho_2 = 0.08, q_1 = 20, q_2 = 100$ ), Fig. 3a illustrates the motion trails of the robots (black dots) relative to the true target positions (red squares) and the estimated target positions (blue translucent squares) as the simulation progresses. As seen, the robots approach the targets while accounting for the risk of detection and failures (depicted by the shaded purple regions). We now compare the performance of our controller with and without the risk aware piece. The latter behavior is simulated by removing the constraint (17e) as well as the second term in (17a). In this scenario, the robots drive close to the targets in an attempt to obtain accurate estimates of the target positions (see Fig. 3b). Figure 4 compares the tracking performance and sensor margin over the course of the experiment, and indicates the times at which the sensor failures occurred. As seen, without accounting for the detrimental effects of future failures, the robots drive very close to the targets, consequently experiencing a much larger rate of sensor failures, which ultimately renders the target tracking system unobservable (hence ending the experiment early). The average mean-squared target estimation errors corresponding to the risk-aware and non-risk-aware experiments was 1.08 and 1.90, respectively, demonstrating the ability of our risk-aware adaptive controller to preserve

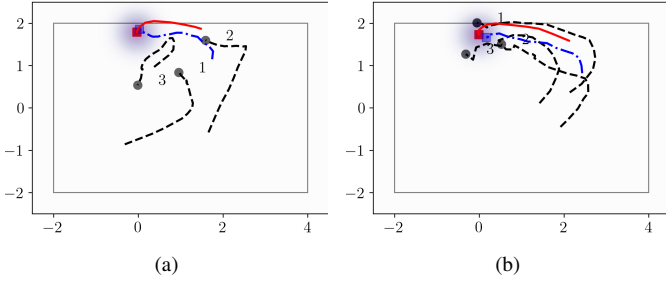


Fig. 3. Heterogeneous target tracking experiment: Motion trails of the quadrotors (black dots), mobile ground target (red square), and estimated target location (blue translucent square). The target risk field is illustrated by the shaded region around the target. (a) illustrates how the risk-aware constraint (17e) enables the robots to trade-off between current and future tracking performance by maintaining a distance from the target. This can be contrasted with the behavior in (b) where the risk-aware constraint has been removed.

sensors and continue operating for a longer period of time with a lower overall tracking error.

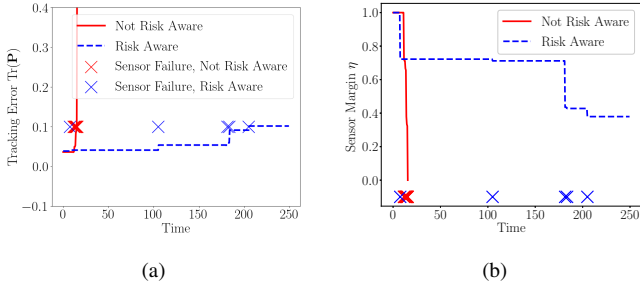


Fig. 4. Comparison of total tracking error with and without the risk aware controller encoded in constraint (17e). In the case where future performance is not accounted for, the larger number of sensor failures dramatically increases the tracking error of the robots (see (a)). This corresponds to a decreasing sensor margin as seen in (b) and a mean-squared tracking error of 1.90. In contrast, the proposed risk-aware adaptive controller enables the multi-robot team to track the targets for a longer time horizon, and maintains a larger sensing margin  $\eta$  over the simulation time horizon, keeping the mean-squared tracking error at 1.08.

For the second set of experiments, we consider a team of 4 simulated robots tracking 2 targets. The robots are equipped with the same types of sensors described in (9). The robots are simulated as ground robots operating in  $\mathbb{R}^2$ , with single integrator dynamics:  $\dot{\mathbf{x}} = \mathbf{u}$ , where  $\mathbf{x}$  denotes the positions of the robots. We assign the following sensor matrix for the team at deployment time:  $\gamma_1 = [1, 2, 3]$ ,  $\gamma_2 = [1, 2, 3]$ ,  $\gamma_3 = [3]$ ,  $\gamma_4 = [1, 2]$ . For the parameters ( $d_m = 0.33$ ,  $d_n = 2.0$ ,  $c_j = 3$ ,  $\Sigma_j = \text{Diag}([4.0, 4.0])$ ,  $j \in \{1, 2\}$ ,  $\rho_1 = [0.45, 0.45]$ ,  $\rho_2 = 0.1$ ,  $q_1 = 1$ ,  $q_2 = 600$ ), Fig. 5 compares the performance of the algorithm with and without the risk-aware constraint (17e). In particular, we present the averaged results over 10 simulation runs to demonstrate the consistent performance of the developed framework. As seen, not only does the proposed framework ensure the longer operability of the robot team, the variance in the tracking performance is also lower when compared to the case with no risk-awareness. The average solve time for the optimization

program was 0.03 seconds for the 3 robots, 1 targets case, and 0.6 seconds for the 4 robot, 2 targets case.

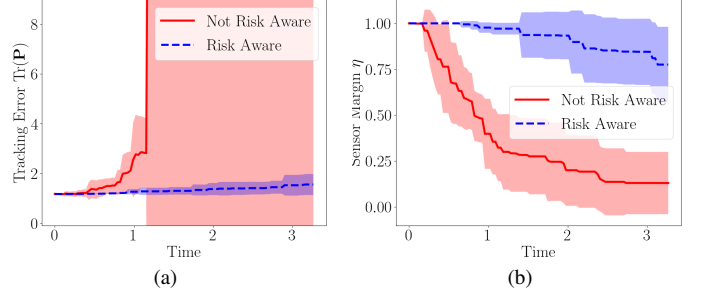


Fig. 5. Performance of the proposed controller in the face of target-induced failures (4 robots, 2 targets). Similar to Fig. 4, the addition of the risk-aware component allows a balance between performance maximization and the quality of future measurements—allowing for better performance over a longer time horizon. The solid lines denote the mean values (over 10 simulation runs), and the shaded region depicts the  $\pm 1$  standard deviation. Note that, in (a), the variance over the simulation runs is lower in the case of the risk-aware controller.

Fig. 6 compares the team-wide tracking error  $\text{Tr}(\mathbf{P})$  and the risk metric  $\text{Tr}(\mathbf{O}_{\Pi}^{-1})$  for varying sensor margin values. From Fig. 6, it is interesting to observe that the system prioritizes performance over safety when the measure of observability of the tracking system is high, and vice versa. Note that, to illustrate this point, the sensor margin  $\eta$  was not computed using (16) but was directly specified to the optimization program which then generated the robot configurations accordingly.

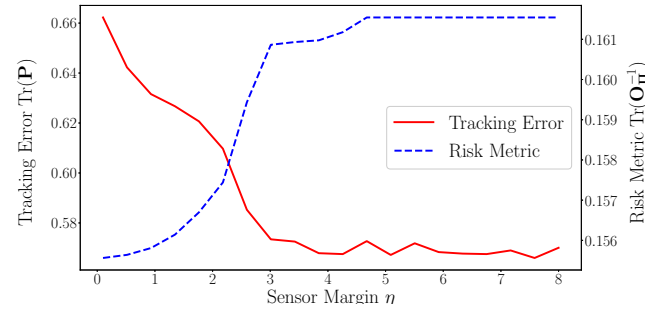


Fig. 6. The automatic trade-off between performance and risk-aversion within the proposed control framework as a function of the sensor margin of the team  $\eta$ . Thanks to the cost functions in (17), the optimization-based controller inherently prioritizes performance for high sensor margins, and prioritizes safety as the sensor margin decreases.

In order to compare the proposed controller against canonical safety-aware control techniques used in the literature (see Section II), we implemented an artificial potential-field (APF) based control algorithm which follows the targets while also maintaining a safe distance from them. The robots are modeled using double-integrator dynamics ( $\ddot{\mathbf{x}} = \mathbf{u}$ ). In particular, a scaled version of (18) is considered as the repulsive APF, and quadratic Euclidean distance-based model is chosen as the attractive APF, similar to [12].

For 2 targets and 3 robots starting in the same configuration, Fig. 7 compares the performance of the two approaches

over 10 simulation runs. Note that, the tracking accuracy performance of both methods is identical in the beginning of the simulation, when no sensing failures have occurred. The differences arise as sensor failures start to occur—since the potential field method is not adaptive, the robots simply continue to maintain the same distance from the targets and experience constant sensor failures. On the other hand, the developed framework adapts to the decreasing sensor margin, by placing different agents at different distances from the targets. This enables the robot team to operate for much longer.

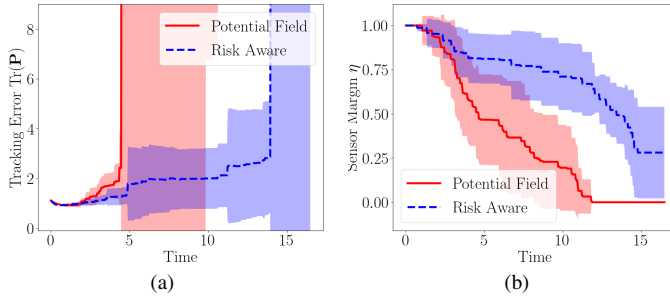


Fig. 7. Comparison of proposed framework with an APF-based baseline controller designed to track targets while maintaining a safe distance from them (3 robots, 2 targets). The proposed risk-aware controller actively reacts to ongoing failures, and hence allows the robot team to remain operational for a much longer period of time.

## VI. CONCLUSION

We present a framework which explicitly trades off between risk and tracking performance while exploiting heterogeneity in the sensors within the robot team. A systematic way to reason about this heterogeneity is provided, which enables the optimization of the current and future tracking performance of the team. While the experiments in the paper used specific examples of heterogeneity and risk models, our framework is general and can be utilized with more complex models as well. Real robot experiments demonstrate ability of this framework to extend the operating lifespan of a target tracking system of robots in hazardous conditions.

## REFERENCES

- [1] A. Ulusoy, S. L. Smith, X. C. Ding, and C. Belta, "Robust multi-robot optimal path planning with temporal logic constraints," in *2012 IEEE International Conference on Robotics and Automation*. IEEE, 2012, pp. 4693–4698.
- [2] W. Luo and K. Sycara, "Minimum k-connectivity maintenance for robust multi-robot systems," in *2019 IEEE/RSJ International Conference on Intelligent Robots and Systems (IROS)*. IEEE, 2019, pp. 7370–7377.
- [3] K. Zhou and J. C. Doyle, *Essentials of robust control*. Prentice hall Upper Saddle River, NJ, 1998, vol. 104.
- [4] L. F. Chamon, A. Amice, S. Paternain, and A. Ribeiro, "Resilient control: Compromising to adapt," in *2020 59th IEEE Conference on Decision and Control (CDC)*. IEEE, 2020, pp. 5703–5710.
- [5] Y. Rizk, M. Awad, and E. W. Tunstel, "Cooperative heterogeneous multi-robot systems: A survey," *ACM Computing Surveys (CSUR)*, vol. 52, no. 2, pp. 1–31, 2019.
- [6] E. Sless, N. Agmon, and S. Kraus, "Multi-robot adversarial patrolling: facing coordinated attacks," in *Proceedings of the 2014 international conference on Autonomous agents and multi-agent systems*, 2014, pp. 1093–1100.
- [7] M. Schwager, P. Dames, D. Rus, and V. Kumar, "A multi-robot control policy for information gathering in the presence of unknown hazards," in *Robotics research*. Springer, 2017, pp. 455–472.
- [8] R. K. Ramachandran, P. Pierpaoli, M. Egerstedt, and G. S. Sukhatme, "Resilient monitoring in heterogeneous multi-robot systems through network reconfiguration," *IEEE Transactions on Robotics*, vol. 38, no. 1, pp. 126–138, 2022.
- [9] B. Friedland, "Controllability index based on conditioning number," *Journal of Dynamic Systems, Measurement, and Control*, vol. 97, no. 4, pp. 444–445, 1975.
- [10] L. Zhou, V. Tzoumas, G. J. Pappas, and P. Tokekar, "Resilient active target tracking with multiple robots," *IEEE Robotics and Automation Letters*, vol. 4, no. 1, pp. 129–136, 2018.
- [11] Z. Zhang and P. Tokekar, "Tree search techniques for adversarial target tracking with distance-dependent measurement noise," *IEEE Transactions on Control Systems Technology*, 2021.
- [12] E. Seraj and M. Gombolay, "Coordinated control of uavs for human-centered active sensing of wildfires," in *2020 American Control Conference (ACC)*. IEEE, 2020, pp. 1845–1852.
- [13] H. X. Pham, H. M. La, D. Feil-Seifer, and M. Deans, "A distributed control framework for a team of unmanned aerial vehicles for dynamic wildfire tracking," in *2017 IEEE/RSJ International Conference on Intelligent Robots and Systems (IROS)*. IEEE, 2017, pp. 6648–6653.
- [14] L. Wang, A. D. Ames, and M. Egerstedt, "Safety barrier certificates for collisions-free multirobot systems," *IEEE Transactions on Robotics*, vol. 33, no. 3, pp. 661–674, 2017.
- [15] A. A. Adepegb, S. Miah, and D. Spinello, "Multi-agent area coverage control using reinforcement learning," in *The Twenty-Ninth International Flairs Conference*, 2016, pp. 368–373.
- [16] J. Votion, T. Feng, and Y. Cao, "Risk-aware multi-agent path planning for target detection: A multi-agent reinforcement learning approach," in *AIAA Scitech 2021 Forum*, 2021, p. 0267.
- [17] R. N. Haksar and M. Schwager, "Distributed deep reinforcement learning for fighting forest fires with a network of aerial robots," in *2018 IEEE/RSJ International Conference on Intelligent Robots and Systems (IROS)*. IEEE, 2018, pp. 1067–1074.
- [18] K. Saulnier, D. Saldana, A. Prorok, G. J. Pappas, and V. Kumar, "Resilient flocking for mobile robot teams," *IEEE Robotics and Automation letters*, vol. 2, no. 2, pp. 1039–1046, 2017.
- [19] R. K. Ramachandran, N. Fronda, and G. S. Sukhatme, "Resilience in multi-robot target tracking through reconfiguration," in *2020 IEEE International Conference on Robotics and Automation (ICRA)*. IEEE, 2020, pp. 4551–4557.
- [20] J. Song and S. Gupta, "Care: Cooperative autonomy for resilience and efficiency of robot teams for complete coverage of unknown environments under robot failures," *Autonomous Robots*, vol. 44, no. 3, pp. 647–671, 2020.
- [21] S. Arosh, S. Nayak, S. Dutttagupta *et al.*, "Fitness function based sensor degradation estimation using h infinity filter," *Procedia Computer Science*, vol. 58, pp. 172–177, 2015.
- [22] J. P. Hespanha, *Linear systems theory*. Princeton university press, 2018.
- [23] L. A. Aguirre, L. L. Portes, and C. Letellier, "Structural, dynamical and symbolic observability: From dynamical systems to networks," *PLoS One*, vol. 13, no. 10, p. e0206180, 2018.
- [24] P. E. Gill, W. Murray, M. A. Saunders, and E. Wong, "User's guide for SNOPT 7.7: Software for large-scale nonlinear programming," Department of Mathematics, University of California, San Diego, La Jolla, CA, Center for Computational Mathematics Report CCoM 18-1, 2018.
- [25] R. Tedrake and the Drake Development Team, "Drake: Model-based design and verification for robotics," 2019. [Online]. Available: <https://drake.mit.edu>
- [26] D. Thakur, Y. Tao, R. Li, A. Zhou, A. Kushleyev, and V. Kumar, "Swarm of inexpensive heterogeneous micro aerial vehicles," in *International Symposium on Experimental Robotics*. Springer, 2020, pp. 413–423.
- [27] N. Michael, J. Fink, and V. Kumar, "Experimental testbed for large multirobot teams," *IEEE robotics & automation magazine*, vol. 15, no. 1, pp. 53–61, 2008.
- [28] R. Mehra, "On-line identification of linear dynamic systems with applications to kalman filtering," *IEEE Transactions on Automatic Control*, vol. 16, no. 1, pp. 12–21, 1971.